Performance Enhancement of Dye Sensitized Solar Cell (DSSC) through TiO_2/rGO Hybrid: Comprehensive Study on Synthesis and Characterization

Rustan Hatib[1]*, Khairil Anwar[1], Ramang Magga[1], Muh Anjas Astak[1], Denny Widhiyanuriyawan[2], Wardoyo[3]

[1]*Mechanical Engineering, Tadulako University, Jl. Soekarno Hatta, Palu, 94119, Indonesia*
[2]*Mechanical Engineering, Brawijaya University, Jl. MT Haryono, Malang, 65145, Indonesia*
[3]*Mechanical Engineering, Jakarta State University, Jl. Rawamangun Muka Raya, Jakarta, 13220, Indonesia*
**Corresponding author: rustanhatib98@gmail.com*

Article history:
Received: 1 June 2024 / Received in revised form: 4 July 2024 / Accepted: 9 July 2024
Available online 18 July 2024

ABSTRACT

The TiO_2 film is immersed in a graphite oxide solution, preparing it for thermal reduction, which converts the graphite oxide to reduced graphene oxide (rGO). This process produces rGO hybrid TiO_2 photoanodes for dye-sensitized solar cells (DSSC). rGO in the TiO_2 structure prevents electron recombination and improves overall efficiency. The main advantage of this method is its ability to prevent loss of rGO during the sintering process, which is a common problem with other methods. The study investigated heating temperatures ranging between 300˚C, 350˚C, 400˚C, 450˚C, and 500˚C to determine optimal conditions. The presence of rGO in the photoanode structure was confirmed via X-ray diffraction and Fourier transform infrared spectroscopy analysis. JV (current-voltage density) measurements of DSSC based on TiO_2/rGO photoanode revealed that the highest photoelectric conversion efficiency (0.1923%) was achieved at 400˚C, much higher than other temperature variations. The findings demonstrate the effectiveness of a simple low-temperature thermal reduction process in producing graphene suitable for semiconductor applications in DSSC. The RGO produced through this method not only improves energy conversion efficiency but also outperforms traditional graphite electrodes. By optimizing the thermal reduction process and fine-tuning the heating conditions, this study advances the practical application of graphene-based materials in solar cell technology. This method overcomes the loss of rGO during sintering, ensuring its beneficial properties are retained. Overall, this study shows that low-temperature thermal reduction is an efficient technique to improve DSSC performance through the incorporation of reduced graphene oxide.

Keywords: *DSSC, efficiency, hybrid, rGO*

I. Introduction

Currently, solar energy is the best choice to answer the challenges of current global energy needs, with photovoltaic technology as the main solution [1], [2]. Photovoltaic technology, which never runs out of resources, can convert sunlight into electricity through photovoltaic (PV) cells. Among all renewable energy technologies, photovoltaic technology is very attractive for directly converting sunlight into high-quality electrical energy. However, existing silicon-based solar cells are limited to the terrestrial PV market due to high production and environmental costs. Compared with high-cost conventional silicon solar cells, dye-sensitive solar cells (DSSC) are known as cost-effective photovoltaic devices due to their cheap materials and simple fabrication process [3].

In 1985, Graetzel and his team researched the sensitivity of polycrystalline TiO_2 electrodes (anatase phase) using the Ru-bipyridine complex. Over the next thirty years, these

DOI: 10.17977/um016v8i12024p138

efforts drove significant academic exploration and technological breakthroughs in understanding the mechanisms of DSSC. The basic configuration of a DSSC consists of three main elements: a dye coupled to a nanocrystalline TiO_2 photoanode, an electrolyte solution hosting a redox agent, and a Pt counter cathode, which offers a cost-effective solution with acceptable energy conversion efficiency. This makes them competitive with silicon-based solar cell technologies. However, the high cost of Pt used in all DSSC cathodes has led to efforts to reduce device costs. Nano, micro carbon, and carbon nanotubes have become attractive alternatives to DSSC electrodes [4], [5].

Various efforts have been made to improve DSSC efficiency. These efforts include improving performance through the addition of nano-sized nanoparticles to the semiconductor layer structure, as seen in Hu's research in [6], which deposits Ag nanoparticles. The use of Indium nanoparticle doping is carried out by [7], and the addition of bamboo charcoal powder particles. Materials with semiconducting properties, such as TiO_2 and reduced graphene oxide (rGO), can potentially increase solar cells' efficiency. The operating mechanism of DSSC includes light absorption by dye molecules and charge separation by inorganic semiconductor nanocrystals with a wide band gap, such as TiO_2. The thickness of the TiO_2 layer deposited on the substrate is greatly influenced by the number of TiO_2 particles distributed on it. The more TiO_2 particles that are distributed, the more dye molecules can be deposited. The dye molecules distributed on the substrate function as photosensitizers, which can stimulate electrons when exposed to photons. The usefulness of TiO_2 is mainly because it has a porous structure, which increases the absorption of dyes, thereby increasing the efficiency of DSSC. However, it should be remembered that the porous structure can also inhibit charge transfer between TiO_2 particles because the transfer process is random, as explained in [9].

To overcome the random displacement of TiO_2, the solution is to add rGO. RGO has outstanding electrical, thermal, and mechanical characteristics. The unique structure of rGO brings improvements to the properties of GO. The extraordinary advances in both the optical and mechanical properties of rGO open up great potential in various applications[10]. Latest research by [11], utilization of rGO as a Hole Transport Layer (HTL) in perovskite solar cells is illustrated, highlighting its potential to increase efficiency. RGO is produced via thermal reduction of GO and can act as a catalyst, as has been researched by [12], when they considered GO and NiO as Double HTL layers in PSC. rGO can be used as a composite because it has a band gap value that is smaller than the band gap of TiO_2, namely (1.00 – 1.69 eV) [13]. In this study, the addition of GO as HTL prevents current recombination and functions as a barrier layer, thereby increasing the filling factor and PSC efficiency. In the same study, TiO_2 was mixed with rGO to avoid recombination between electrons and dye, thereby increasing DSSC efficiency.

In previous studies, various studies have been carried out to explore rGO/TiO_2 blending in the context of DSSC. This study includes a variety of sintering methods to understand how temperature differences affect DSSC structure and efficiency. However, in this study, we focused on analyzing differences in sintering temperatures using the same sample for each temperature variation. This approach allows researchers to explore further the specific influence of each sintering temperature on the characteristics and performance of rGO/TiO_2-based DSSC.

The study's novelty lies in the low-temperature thermal reduction method used to prepare rGO, which prevents the loss of rGO during the sintering process, a common

problem with other methods. This approach ensures that the beneficial properties of rGO are maintained, thereby improving electron transport and reducing recombination.

The thermal reduction process produces graphene by reducing GO. This study explores the properties of graphene produced using this approach, as well as its electrical properties and catalytic potential. Graphene produced via low-temperature thermal reduction is used as a semiconductor material in the ongoing development of DSSC. Electrode performance was assessed using X-ray diffraction (XRD) and Fourier transform infrared spectroscopy (FT-IR), as well as measurement of DSSC photovoltaic characteristics. The findings of this study demonstrate that a direct method for reducing GO at low temperatures effectively produces graphene suitable for use as a semiconductor material in DSSC. Moreover, graphene shows higher energy conversion efficiency than graphite.

The main objective of this study is to investigate the impact of sintering temperature variations on the structural, chemical, and electrical properties of rGO/TiO_2-based DSSC and to optimize the conditions to achieve the highest possible efficiency. This study involves advancing the practical application of graphene-based materials in solar cell technology, addressing the challenges of electron recombination, and improving the overall performance of DSSC.

II. Materials and methods

1. Materials

DSSC was made using different materials: TiO_2 nanopowder (Degussa P25, USA), Iodine (I_2) (Merck, Germany), potassium iodide (KI) (Merck, Germany), and carbon (candle tip). Fluorine-doped Tin Oxide coated glass slide (FTO) (Merck, Germany). Ethanol and acetone were purchased from (BDH, UK). Natural coloring extracted from Moringa leaves (Central Sulawesi, Indonesia)

2. Preparation of the electrode

The stages of making a working electrode are as follows:

A. Fluorine-doped Tin Oxide (FTO) glass cleaning

The material generally used is FTO; this material is used because, in the process of coating TiO_2 material onto a substrate, a sintering process at 400-500˚C is required. This material is suitable because it does not experience defects in this temperature range. Take the prepared FTO glass and pour 200 ml of 96% ethanol into the beaker. Use tweezers to insert the FTO beaker into the beaker containing ethanol. This step aims to clean the glass from other potential materials that might stick to the glass surface [14].

B. Making TiO_2 Paste

The process of making TiO_2 (paste) is carried out according to the amount needed based on the amount of glass used. TiO_2 powder was mixed with 15 ml of ethanol and then stirred using a magnetic stirrer for approximately 30 minutes until completely dissolved. Continue stirring the solution until it reaches a homogeneous, thickened consistency. After the cooling process, TiO_2 paste is ready to use [18].

C. The process of making rGO from graphite

RGO is made by the hydrothermal method. Graphene oxide was dispersed in ethanol and deionized water by ultrasonic treatment for 1 h. The suspension was placed in a 100 mL Teflon-sealed autoclave and heated at 180 °C for 8 hours. Finally, rGO powder was prepared

after the samples were dried in air under ambient conditions (Figure 1) [16]. The dried photoanode is then introduced into a tube furnace under an argon atmosphere. The temperature gradually increased from 300˚C to 500˚C, with each temperature level maintained for one hour to sinter the photoanode. The final product consists of a TiO_2 photoanode decorated with rGO [17]. They were then designated as rGO-300˚C, rGO-350˚C, rGO-400˚C, rGO-450˚C, and rGO-500˚C respectively.

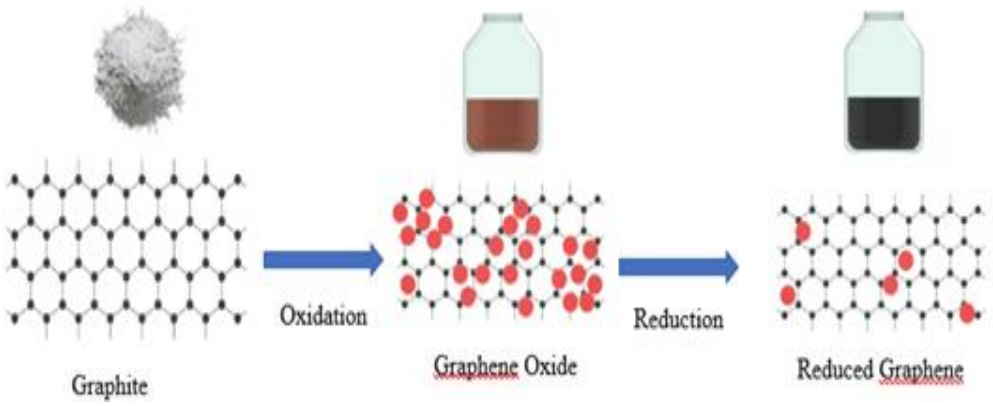

Fig. 1. Graphene oxide process for reducing graphene oxide

D. Precipitate

TiO_2/rGO paste will be deposited using the doctor blade technique on a conductive area of FTO glass measuring 2 x 2 cm^2. Scotch tape will be attached as a barrier to the conductive surface. Using a dropper pipette, a few drops of TiO_2/rGO paste will be applied to the surface of the conductive glass, and the fine part of the pipette will be used to spread a layer of TiO_2/rGO paste over the entire area bounded by the conductive glass. After that, let it sit for a few minutes until it dries, as in Figure 2.

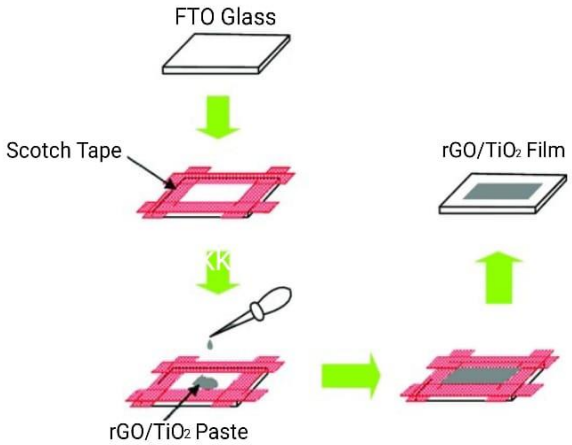

Fig. 2. Illustration of the TiO_2/rGO paste deposition process

The next step is sintering on a hotplate with temperatures ranging from 300˚C to 500˚C for approximately 45 minutes. At the sintering stage, TiO_2/rGO will change color to brown,

then return to white. The success of the sintering process can be confirmed when the TiO_2 is white again. Before removing, leave for ± 5 minutes or until completely cold.

e. Soaking in Dye

If the sintering process has been successful, the next step is to soak the TiO_2 layer in a dye solution made from pure Moringa leaf extract. This soaking process lasts for 24 hours, ensuring the TiO_2 layer is thoroughly saturated with the dye. After soaking, the layer can be further processed as required.

f. Electrolyte Manufacturing

The electrolyte was prepared as follows: electrolyte solution was made by dissolving a mixture of 0.8 grams (0.5 M) of potassium iodide (KI) into 10 ml of PEG 400 and then stirring evenly. Furthermore, 0.127 grams (0.05 M) of iodine (I2) was added to the solution and stirred until all three ingredients were completely dissolved. The ready-to-use electrolyte solution was temporarily stored in an enclosed dark bottle [18].

3. Making Carbon Electrodes

Making a counter electrode involves heating the conductive side of the glass over candle soot until it appears black. This process results in the formation of a carbon layer. One of the FTO glass substrates that functions as a counter electrode is heated with a candle flame until soot covers the conductive area of the substrate. This heating process makes the substrate coated with carbon, which acts as a catalyst in DSSC. This catalyst is needed to speed up the reaction kinetics in the reduction process in FTO.

4. DSSC Assembly

Create a sandwich layer by adjusting the offset of the working electrode with the counter electrode. Assembly was carried out with the two electrodes attached using a paper clip for further testing regarding DSSC efficiency. The material arrangement in DSSC is shown in Figure 3.

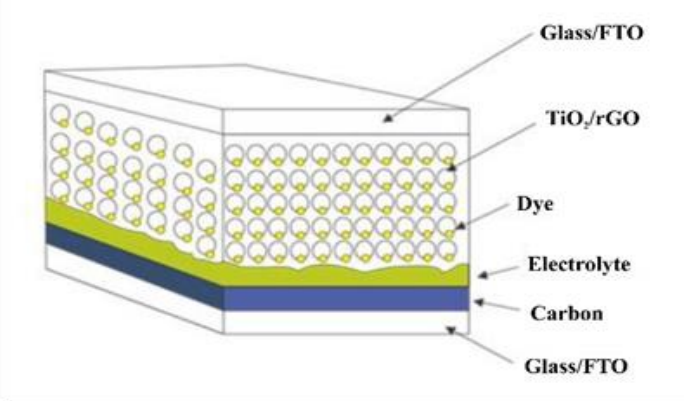

Fig. 3. Illustration of the assembled DSSC [18]

5. Measurement of DSSC Photoelectric Conversion Efficiency

a. Power Measurement

The power produced by solar cells is expressed in Eq. (1). They are influenced by the active cross-sectional area of the DSSC because it determines the intensity of the light absorbed.

$$Pin = I\ x\ A \quad \text{..... (1)}$$

Where:

Pinput: Power absorbed from the light source (mW)
I : Light intensity (mW/cm^2)
A : Active surface area (cm^2)

b. Fill factor measurement

Fill Factor is the ratio of maximum output power to short circuit current and open circuit voltage. So DSSC efficiency is calculated using Eq. (2):

$$FF = \frac{Jmaks\ X\ Vmaks}{Jsc\ X\ Voc} \quad \text{.....(2)}$$

Where:

FF : Fill factor
Imax : Maximum current (mA)
Vmax : Maximum voltage (mV)
Isc : Short circuit current (mA)
Voc : Open network voltage (mV)

By using Fill Factor, the maximum power of the solar cell is obtained from the Eq. (3):

$$Pout = Jsc\ x\ Voc\ x\ FF \quad \text{.....(3)}$$

Where:

Pout : Power generated (mW)
Voc : Open network voltage (mV)
Isc : Short circuit current (mA)
FF : Fill factor

So the efficiency of a solar cell is generated from the power obtained from the cell (Pout) divided by the incoming light power (Pin) (Eq. 4), namely the power that comes from the sun with a certain intensity.

$$\eta = \left(\frac{Pout}{Pin}\right) x\ 100\% \quad \text{.....(4)}$$

Where:
η : Efficiency (%)
Pout : Power produced (mW)
Pin : Power absorbed from the light source (mW)

3. Results and Discussion

1. FT-IR Analysis

As seen in Figure 4, the peak is greatly broadened, and its intensity is parallel to the OH stretching vibration at about 3440 cm^{-1}, indicating the presence of a large amount of H_2O or OH adsorbed on the synthesized carboxylate groups in the GO sample [19]. The thermal reduction process results in the stabilization of the carbon base plane, which is indicated by the symmetric and asymmetric vibration of the CH_2 group, observed at the peak position of 2865 cm^{-1}[20], [21].

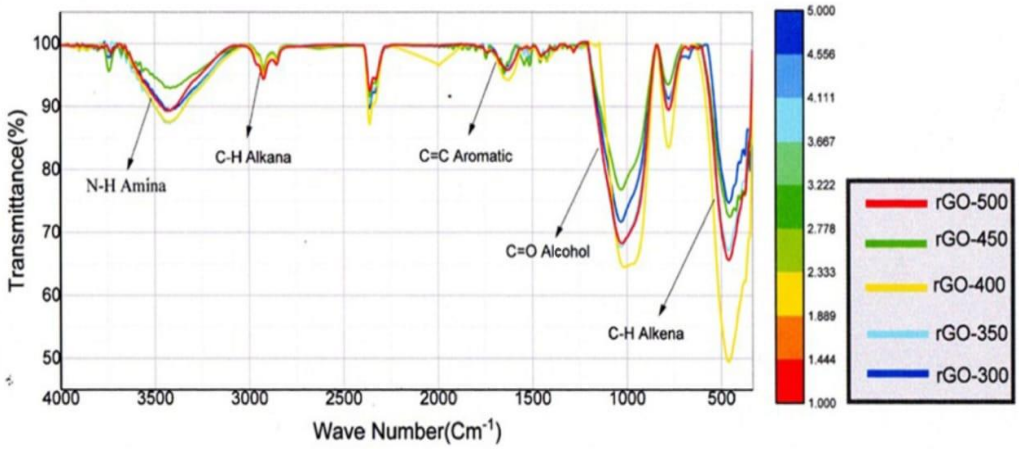

Fig. 4. Functional groups in DSSC

In addition, the occurrence of impurities such as CO, C=O, and C-OH groups in the carbon substrate indicates the prevalence of many oxygen-containing functional groups in GO. These peaks disappeared after thermal annealing. Therefore, it was concluded that GO is unsuitable as a semiconductor material because it contains many impurities and cannot conduct electricity. However, through high temperature heating during heat treatment, the residue can be removed. The resulting thermal desolvation products, which originate from heating GO, were assessed for their electrical conductivity as a semiconductor material in DSSC. The shift in peak positions in XRD analysis and identification of interphase impurities via FT-IR can also explain the resistance behavior of GO. When GO is heated, the presence of oxygen and functional groups affects its electrical conductivity, which worsens the charge transfer in DSSC. The reduction in oxygen content identified through FT-IR measurements suggests that thermal reduction methods can overcome these oxygen-related defects.

The tests used in the spectrum range 500 – 4000 cm^{-1}. Figure 4 shows that in the wave number in the range 1500 cm^{-1}– 500 cm^{-1}, there are CH (Alkene) bonds. In the wave number 1300 cm^{-1}– 1000 cm^{-1}, there are C=O bonds (Alcohols). In wave numbers 2000 cm^{-1} – 1500 cm^{-1}, there are C=C bonds (Aromatics). In wave numbers 3000 cm^{-1}- 2800 cm^{-1}, there are CH bonds (Alkanes), and in wave numbers 3600 cm^{-1} – 3300 cm^{-1}, there are NH (amine) bonds. The FT-IR test results show an absorption intensity in the FT-IR spectrum wave. The sharper the wave number in the FT-IR spectrum, the higher the structure or carbon groups formed. This shows that the greater the energy absorbed by the functional groups formed. Based on the data above, the highest spectral wave absorption at the sintering temperature is 400˚C which has a spectral wavelength of 3439.07 cm^{-1} [3].

The bonds at the sintering temperature are hydroxyl (OH), appearing in the wave number range of 3600-3300 cm^{-1}. The IR spectrum of the rGO/TiO_2 nanocomposite exhibits a characteristic wide peak at a wave number of 3367 cm^{-1}. This peak corresponds to the OH vibration path.

2. XRD Analysis

Figure 5 displays the XRD pattern of the TiO_2/rGO photoanode, analyzed in the angular range 2θ = 20 to 80° using XRD. Sample examination was carried out using an X-ray

diffractometer with a scanning speed of 5 minutes. The diffraction patterns indicate an important degree of crystallinity for all materials present in the photoanode [22].

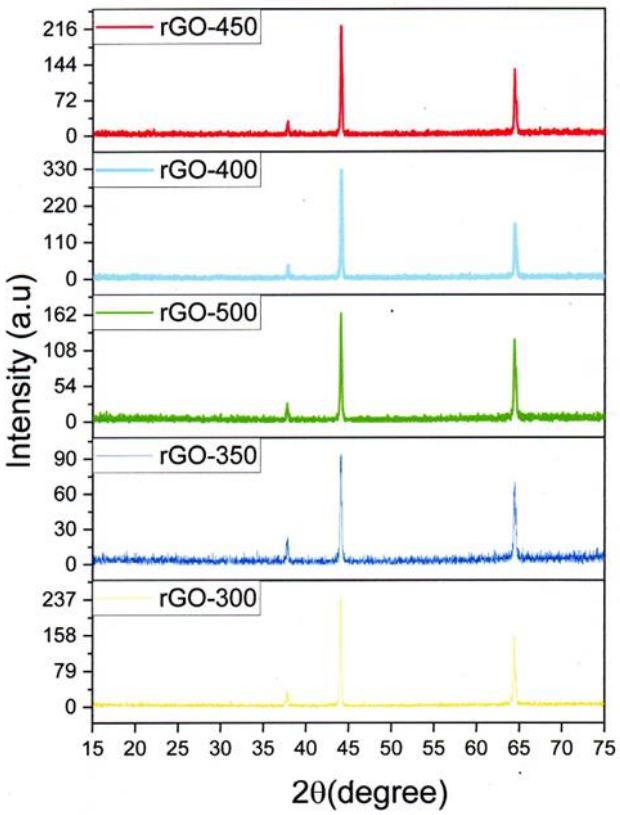

Fig. 5. XRD test results for each heating variation

Figure 5 illustrates the anastase phase at a sintering temperature of 300^{o}C occurs at diffraction angles of 44.031°, 64.410°, and 37.782°; Sintering temperature of 350^{o}C at angles 44.055°, 64.426°, and 37.790°; Sintering temperature of 400^{o}C with angles 44.051°, 64.422°, and 37.813°. Sintering temperature 450^{o}C with angles 44.041°, 64.405°, and 37.763°; Sintering temperature 500^{o}C with angles 44.067°, 64.437°, and 37.426°. The highest angles were found at a sintering temperature of 400^{o}C, namely at angles 44.051°, 64.422°, and 37.813°.

Figure 5 illustrates the XRD pattern depicting the temperature changes observed during the thermal reduction process of GO to graphene powder (GP). It can be observed that graphene oxide, graphite oxide, and GP heating all have peaks that appear in the series Peak 1, Peak 2, and Peak 3, which initially have a narrower d range that will undergo oxidation to graphite oxide. Then, in turn, it undergoes oxidation to become graphene oxide. At this point, many impurities are introduced into the carbon layer, causing the largest d-spacing in GO. Thermal reduction helps remove impurities by providing heat energy during the GO reduction process. This process introduces functional groups and impurities, such as water molecules, carboxyl groups, hydroxyl groups, and epoxy groups, into the GP material through the applied thermal reduction temperature. Therefore, the removal of impurities from the GO layer causes the rearrangement of the graphene and the narrowing of the d-gap.

The lack of graphite crystal peaks at 38° indicates that the graphite has completely transformed into graphene oxide (Peak series 1). After thermal reduction, the peak shifts to the right, indicating a decrease in the interlayer distance with increasing thermal temperature, reaching about 0.35 nm [23], [24]. These observations suggest that thermal processes can remove oxygen and water between the layers. However, the presence of graphite oxide intermediates, as seen in the Peak 2 series, indicates that Hummers' method does not completely convert graphite to graphene oxide. Scherrer's equation can be used to determine the size of GP crystals by measuring the full width at half maximum (FWHM) at Peak 3. The FWHM decreases slightly as temperature increases, indicating that further decreasing temperature can enlarge the size of GP by removing impurities and promoting crystallization.

Analysis of the XRD test results on the DSSC crystal structure shows that the addition of rGO to TiO_2 affects the diffraction pattern and crystal structure formed. At a sintering temperature of 400°C, the sharp diffraction peaks indicate that the TiO_2 anatase structure reaches the highest degree of order. The shift and broadening of the diffraction peaks after adding rGO indicate a distortion in the TiO_2 crystal lattice, which increases the total surface area and electron transfer pathways.

The more regular crystal structure at the optimal sintering temperature of 400°C is directly related to the highest efficiency achieved by DSSC, namely 0.1923%. The good crystal structure and presence of rGO help reduce electron recombination, thereby increasing the efficiency of electron transfer and energy conversion. For comparison, a previous study using a similar method but without the addition of rGO showed an efficiency of only 0.047% with a main diffraction angle of 24.17° [18].

The addition of rGO was proven to significantly improve the crystal structure and performance of DSSC. These results are consistent with other studies stating that modifying the crystal structure by adding additional materials can improve DSSC performance. In this study, the XRD results showed that the addition of rGO changed the crystal structure of TiO_2 and contributed to the improvement of DSSC efficiency. This indicates that rGO plays an important role in enhancing electron transfer and reducing recombination, thereby increasing the overall efficiency of the device.

C. Efficiency Analysis

Performance testing aims to determine the efficiency value based on the current and voltage values that occur. This is done by using heating variations, namely rGO-300˚C, rGO-350˚C, rGO-400˚C, rGO-450˚C, and rGO-500˚C. Heating GO in an inert gas environment to convert it to rGO has been shown to increase the efficiency of DSSC. Thermal processing of GO in an argon atmosphere resulted in the successful reduction of GO to rGO, which was seamlessly integrated into the TiO_2 DSSC photoanode without experiencing any loss. This method is known to induce a phase change in TiO_2 crystals, leading to the creation of mixed crystals within the photoanode. Incorporating rGO with the mixed crystal structure of TiO_2 changes the electronic transmission route, reduces the recombination rate of electron-hole pairs, and consequently increases the DSSC efficiency.

Figure 6 shows that the heating pattern at a temperature of 300 °C provides a current of 17.5 µA and a voltage of 0.488 volts; The temperature of 350 °C provides a current of 11.9 µA and a voltage of 0.609 volts; The temperature of 400 °C, provides a current of 35 µA and voltage of 0.408 volts; The temperature of 450 °C provides current of 17.5 µA and a

voltage of 0.242 volts. Heat 500 °C provides a current of 8.9 µA and a voltage of 0.269 volts.

The presence of rGO in the photoanode is known to impact DSSC efficiency. Table 1 shows that DSSC with optimal rGO heating at a temperature of 400 ˚C at the photoanode exhibits the highest efficiency. This optimal heating has a dual effect on cell performance by facilitating electron transport and reducing electron recombination. However, excessive heating of rGO can cause structural damage to the TiO_2 nanofilm, thereby reducing efficiency.

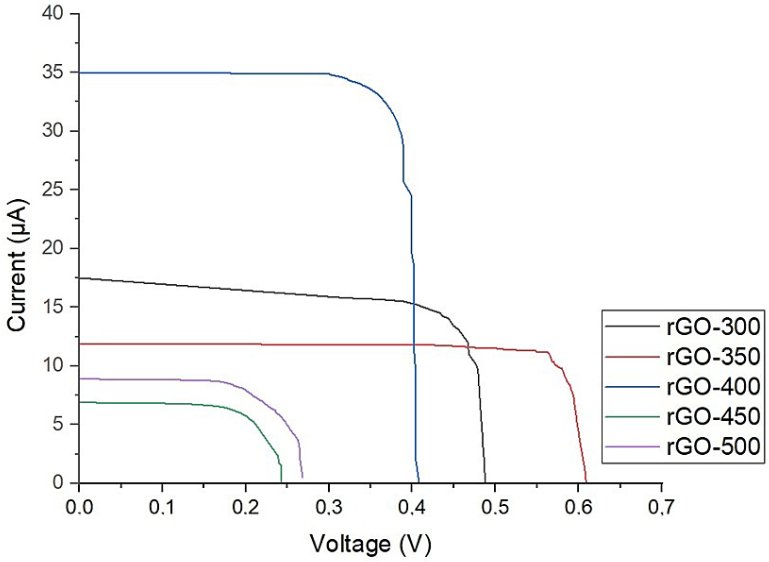

Fig. 6. DSSC I-V curve

Table 1. Comparison of DSSC performance characteristics

NO	Temperature (˚C)	Voc (V)	Isc (µA)	Vmp (V)	Imp (µA)	FF	η (%)
1	300	0.488	17.5	0.434	14.5	0.737	0.1014
2	350	0.609	11.9	0.562	11.2	0.869	0.1015
3	400	0.408	35.0	0.369	32.3	0.834	0.1923
4	450	0.242	17.5	0.434	09.6	0.984	0.0672
5	500	0.269	08.9	0.197	08.1	0.664	0.0257

Thermal reduction of GO to rGO has been shown to change the crystal phase ratio of rutile and anatase in TiO_2, potentially affecting DSSC performance. Incorporation of rGO into the photoanode alters the crystal phase ratio in TiO_2. This change can significantly impact the overall performance of the solar cell. In summary, the thermal reduction of GO to rGO in an inert gas environment positively influences DSSC performance. It modifies the crystal phase ratio, electron transfer pathways, and recombination rate. These changes ultimately result in increased solar cell efficiency.

DSSC efficiency testing involves exposing solar cells to sunlight to produce an electric current through a photoelectrochemical process. Electrons generated from the sensitive dye in TiO_2 will be injected into the counter electrode, producing a current measured during the

test. Current and voltage measurements during experiments are used to calculate solar cell efficiency, reflecting the cell's ability to convert light into electrical energy.

Several factors causing low efficiency in this rGO/TiO_2-based DSSC include significant electron recombination, low light absorption, lower conductivity, charge carrier mobility, and uneven distribution of rGO on TiO_2. However, these low-efficiency DSSC can still be used for low-power applications such as sensors, calculators, small battery charging, and LED lighting, especially in remote or indoor areas, so they have the potential to meet certain electricity needs efficiently.

The addition of reduced rGO to TiO_2 increases electron transfer because rGO has high conductivity and a large surface area, providing a fast path for electrons. RGO acts as an efficient electron transport pathway, reducing electron transit time and the possibility of electron-hole recombination. XRD and FT-IR results confirmed the presence of rGO in TiO_2, while JV measurements showed increased photoelectric efficiency, proving enhanced electron transfer. Other studies, such as the addition of clathrin TiO_2, also show similar results in reducing recombination and increasing efficiency [18].

4. Conclusion

GO was introduced into a hybridized TiO_2 photoanode, followed by thermal treatment in an inert gas atmosphere to convert GO to rGO. The successful doping of rGO into the TiO_2-DSSC photoanode was achieved without loss. By adjusting the heating conditions for rGO/TiO_2, optimal efficiency can be achieved. Further investigations showed that the inclusion of rGO in the photoanode functions not only as a barrier layer but also causes modifications in the crystal phase. This change in crystal structure increases electron transmission in the DSSC and decreases electron recombination. Optimal efficiency is achieved by heating at a temperature of 400˚C. RGO-400˚C based cells showed the best performance, with a short circuit current density (Isc) of 3.5 x 10^{-6} A cm^{-2}, open circuit voltage (Voc) of 0.369 V, fill factor of 0.834, and overall efficiency amounting to 0.1923%.

Reference

[1] Z.A. Ghafour, A.R. Ajel, and N.M. Yasin, "Improvement Performance of Standalone PV System Based on a New Quadratic Boost Converter," *Int. J. Renew. Energy Res.*, vol. 13, no. 1, pp. 481–488, 2023, doi: 10.20508/ijrer.v13i1.13475.g8706.

[2] A.B. Al-Aasam, A. Ibrahim, K. Sopian, M.B. Abdulsahib, and M. Dayer, "Enhancing the Performance of Photovoltaic Thermal Solar Collectors using Twisted Absorber Tubes and Nanofluids with Optimal Design Parameters," *Int. J. Renew. Energy Res.*, vol. 13, no. 3, pp. 1277–1284, 2023, doi: 10.20508/ijrer.v13i3.14163.g8799.

[3] J. Gong, K. Sumathy, Q. Qiao, and Z. Zhou, "Review on dye-sensitized solar cells (DSSCs): Advanced techniques and research trends," *Renew. Sustain. Energy Rev.*, vol. 68, no. December 2015, pp. 234–246, 2017, doi: 10.1016/j.rser.2016.09.097.

[4] W.J. Lee, E. Ramasamy, and D.Y. Lee, "Efficient dye-sensitized solar cells with catalytic multiwall carbon nanotube counter electrodes," *J. Mater.*, vol. 1, no. 6, pp. 1145–1149, 2009, doi10.10: 21/am800249k.

[5] P. Kumar. R. Kumar Singh. N. Rawat and P. Barman, "A novel method for controlled synthesis of nanosized hematite (α-Fe2O3) thin film on liquid-vapor interface," *J. Nanoparticle Res.*, vol. 15, no. 4, 2013, doi: 10.1007/s11051-013-1532-6.

[6] H. Hu, J. Shen, X. Cao, H. Wang, Huiru Lv, W. Zhu, and J. Zhao, "Photo-assisted deposition of Ag nanoparticles on branched TiO2nanorod arrays for dye-sensitized

solar cells with enhanced efficiency," *J. Alloys Compd.*, vol. 694, pp. 653–661, 2016, doi: 10.1016/j.jallcom.2016.10.057.

[7] R.K. Chava and M. Kang, "Improving the photovoltaic conversion efficiency of ZnO based dye sensitized solar cells by indium doping," *J. Alloys Compd.*, vol. 692, pp. 67–76, 2016, doi: 10.1016/j.jallcom.2016.09.029.

[8] C.S. Chou, C.Y. Chen, S.H. Lin, W.H. Lu, and P. Wu, "Preparation of TiO_2/bamboo-charcoal-powder composite particles and their applications in dye-sensitized solar cells," *Adv. Powder Technol.*, vol. 26, no. 3, 2015, doi: 10.1016/j.apt.2014.12.013.

[9] X. Fang, M. Li, K. Guo, X. Liu, Y. Zhu, and X. Zhao, "Graphene-compositing optimization of the properties of dye-sensitized solar cells," *J. Alloys Compd.*, vol. 101, pp. 176–181, 2016, doi: 10.1016/j.solener.2013.12.005.

[10] H. Pinto and A. Markevich, "Electronic and electrochemical doping of graphene by surface adsorbates," *J. Alloys Compd.*, pp. 1842–1848, 2016, doi: 10.3762/bjnano.5.195.

[11] R. Hatib, H. Nurkholis, S. Sudjito, and D. Widhiyanuriyawan, "Performance of Perovskite Solar Cell Coated with Graphene Oxide as Hole Transport Layer," *Eastern-European J. Enterp. Technol.*, vol. 1, pp. 36–43, 2021, doi: 10.15587/1729-4061.2021.225420.

[12] D. Widhiyanuriyawan, H. Nurkholish, and R. Hatib, "Nickel oxide/graphene oxide (NiO/GO) as double hole transport layer in perovskite solar cell," *J. Teh. Vjesn.*, vol. 29, no. 6, pp. 1861–1867, 2016, doi: 10.17559/TV-20211212082922.

[13] S.G. Kumar and L.G. Devi, "Review on modified TiO_2 photocatalysis under UV/visible light: Selected results and related mechanisms on interfacial charge carrier transfer dynamics," *J. Phys. Chem. A*, vol. 115, no. 46, pp. 13211–13241, 2011, doi: 10.1021/jp204364a.

[14] R. Hatib, S. Soeparman, D. Widhiyanuriyawan, and N. Hamidi, "Performance of perovskite solar cell coated with graphene oxide as hole transport layer," *Eastern-European J. Enterp. Technol.*, vol. 1, pp. 36–43, 2021, doi: 10.15587/1729-4061.2021.225420.

[15] B. Liu, J. Kou, F. Li, D. Huo, J. Xu, X. Zhou, D. Meng, M. Ghulam, B. Artyom, X. Gao, N. Ma, and D. Han "Lemon essential oil ameliorates age-associated cognitive dysfunction via modulating hippocampal synaptic density and inhibiting acetylcholinesterase," *Aging (Albany. NY).*, vol. 12, no. 9, pp. 8622–8639, 2020, doi: 10.18632/aging.103179.

[16] N. Ahmadi, A. Nemati, and M. Bagherzadeh, "Synthesis and properties of Ce-doped TiO2-reduced graphene oxide nanocomposite," *J. Alloys Compd.*, vol. 742, pp. 986–995, 2018, doi: 10.1016/j.jallcom.2018.01.105.

[17] W. Lv, F. Sun, D. Ming Tang, H.T. Fang, C. Liu, and H.M. Cheng, "A sandwich structure of graphene and nickel oxide with excellent supercapacitive performance," *J. Alloys Compd.*, vol. 21, no. 25, pp. 9014–9019, 2016, doi: 10.1039/c1jm10400d.

[18] D. Widhiyanuriyawan, P. Trihutomo, S. Soeparman, and L. Yuliati, "Zwitterion effect of cow brain protein towards efficiency improvement of dye-sensitized solar cell (DSSC)," *Sci. World J.*, vol. 2020, pp. 1–12, 2020, doi: 10.1155/2020/7910702.

[19] P. Wang, F. He, J. Wang , H. Yu, and L. Zhao, "Graphene oxide nanosheets as an effective template for the synthesis of porous TiO_2 film in dye-sensitized solar cells," *J. Alloys Compd.*, vol. 358, pp. 175–180, 2016, doi: 10.1016/j.apsusc.2015.06.102.

[20] H. Ding, S. Zhang, J.T. Chen, X.P. Hu, Z.F. Du, and Y.X. Qiu, "Reduction of graphene oxide at room temperature with vitamin C for RGO-TiO_2 photoanodes in dye-sensitized solar cell," *J. Alloys Compd.*, vol. 584, pp. 29–36, 2016, doi:

10.1016/j.tsf.2015.02.038.

[21] F.W. Low, C.W. Lai, and Hamid, "Surface modification of reduced graphene oxide film by Ti ion implantation technique for high dye-sensitized solar cells performance," *J. Alloys Compd.*, vol. 43, no. 1, pp. 625–633, 2016, doi: 10.1016/j.ceramint.2016.09.205.

[22] R. Liu, Y. Qiao, Y. Song, and K. Song, "Enhanced Efficiency of dye-sensitized solar cells using rGO@TiO_2 nanotube hybrids," *J. Alloys Compd.*, vol. 34, no. 2, pp. 269–273, 2016, doi: 10.1007/s40242-018-7287-y.

[23] M. Zhu, X. Li, W. Liu and Y. Cui, "An investigation on the photoelectrochemical properties of dye-sensitized solar cells based on graphene-TiO_2 composite photoanodes," *J. Alloys Compd.*, vol. 262, pp. 349–355, 2016, doi: 10.1016/j.jpowsour.2014.04.001.

[24] J. Liu, X. Fu, D.-P. Cao, and L. Mao, "Stacked graphene-TiO_2 photoanode via electrospray deposition for highly efficient dye-sensitized solar cells," *J. Alloys Compd.*, vol. 23, pp. 158–163, 2016, doi: 10.1016/j.orgel.2015.04.021.